Intermembrane Space Proteome of Yeast Mitochondria*[S]

F.-Nora Vögtle‡§, Julia M. Burkhart§¶, Sanjana Rao‡, Carolin Gerbeth‡‖, Jens Hinrichs¶, Jean-Claude Martinou, Agnieszka Chacinska‡‡, Albert Sickmann¶§§, René P. Zahedi¶ ¶¶, and Chris Meisinger‡‖‖[1]**

The intermembrane space (IMS) represents the smallest subcompartment of mitochondria. Nevertheless, it plays important roles in the transport and modification of proteins, lipids, and metal ions and in the regulation and assembly of the respiratory chain complexes. Moreover, it is involved in many redox processes and coordinates key steps in programmed cell death. A comprehensive profiling of IMS proteins has not been performed so far. We have established a method that uses the proapoptotic protein Bax to release IMS proteins from isolated mitochondria, and we profiled the protein composition of this compartment. Using stable isotope-labeled mitochondria from *Saccharomyces cerevisiae*, we were able to measure specific Bax-dependent protein release and distinguish between quantitatively released IMS proteins and the background efflux of matrix proteins. From the known 31 soluble IMS proteins, 29 proteins were reproducibly identified, corresponding to a coverage of >90%. In addition, we found 20 novel intermembrane space proteins, out of which 10 had not been localized to mitochondria before. Many of these novel IMS proteins have unknown functions or have been reported to play a role in redox regulation. We confirmed IMS localization for 15 proteins using *in organello* import, protease accessibility upon osmotic swelling, and Bax-release assays. Moreover, we identified two novel mitochondrial proteins, Ymr244c-a (Coa6) and Ybl107c (Mic23), as substrates of the MIA import pathway that have unusual cysteine motifs and found the protein phosphatase Ptc5 to be a novel substrate of the inner membrane protease (IMP). For Coa6 we discovered a role as a novel assembly factor of the cytochrome *c* oxidase complex. We present here the first and comprehensive proteome of IMS proteins of yeast mitochondria with 51 proteins in total. The IMS proteome will serve as a valuable source for further studies on the role of the IMS in cell life and death. ***Molecular & Cellular Proteomics 11: 10.1074/mcp.M112.021105, 1840–1852, 2012.***

Mitochondria are double-membrane-bound organelles that fulfill a multitude of important cellular functions. Proteomic analysis of purified mitochondria revealed that they contain approximately 1000 (yeast) to 1500 (human) different proteins (1–3). However, the distribution of these proteins among the four mitochondrial subcompartments (outer membrane, inner membrane, matrix, and intermembrane space) has been only marginally studied through global approaches. This is attributed to the high complexity of purifying submitochondrial fractions to a grade suitable for proteomic analysis. The best-studied submitochondrial proteomes comprise the outer membranes of *S. cerevisae*, *N. crassa*, and *A. thaliana* (4–6). The mitochondrial intermembrane space (IMS)[1] represents a highly interesting compartment for several reasons: it provides a redox active space that promotes oxidation of cysteine residues similar to the endoplasmic reticulum and the bacterial periplasm, but unlike cytosol, nucleus, or the mitochondrial matrix where the presence of thioredoxins or glutaredoxins prevents the risk of unwanted cysteine oxidation (7, 8). Furthermore in higher eukaryotes IMS proteins are released into the cytosol upon apoptotic induction, which triggers the activation of a cell-killing protease activation cascade (9, 10). The IMS can also exchange proteins, lipids, metal ions, and various metabolites with other cellular compartments, allowing mitochondrial metabolism to adapt to cellular homeostasis. In particular, the biogenesis and activity of the respiratory chain were shown to be controlled by various proteins of the IMS (11–13). Most of the currently known IMS proteins are soluble proteins; however, some inner membrane proteins have been annotated as IMS proteins as well,

From the ‡Institut für Biochemie und Molekularbiologie, ZBMZ, Universität Freiburg, 79104 Freiburg, Germany; ¶Leibniz-Institut für Analytische Wissenschaften - ISAS - e.V., Dortmund, Germany; ‖Faculty of Biology, Universität Freiburg, 79104 Freiburg, Germany; **Departement de Biologie Cellulaire, University of Geneva, 1211 Geneva, Switzerland; ‡‡International Institute of Molecular and Cell Biology, 02-109 Warsaw, Poland; §§Medizinisches Proteom-Center (MPC), Ruhr-Universität, Bochum, Germany; ‖‖BIOSS Centre for Biological Signalling Studies, Universität Freiburg, 79104 Freiburg, Germany

Received June 15, 2012, and in revised form, August 13, 2012
⌘ *Author's Choice*—Final version full access.
Published, MCP Papers in Press, September 15, 2012, DOI 10.1074/mcp.M112.021105

[1] The abbreviations used are: ACN, acetonitrile; CID, collision induced dissociation; Coa, Cytochrome *c* oxidase assembly; DDM, dodecylmaltoside; IMP, inner membrane protease; IMS, intermembrane space; PD, Proteome Discoverer; PDH, pyruvate dehydrogenase; SCX, strong cation exchange chromatography; SN, supernatant; TOM, translocase of the outer membrane.

such as proteins that are peripherally attached to the inner membrane or membrane proteins that expose enzyme activity toward the IMS (8).

All IMS proteins are encoded in the nuclear DNA and have to be imported after translation in the cytosol (14–19). Two main pathways are known to mediate the import and sorting of proteins into the IMS. One class of proteins contains bipartite presequences that consist of a matrix targeting signal and a hydrophobic sorting signal. These signals arrest the incoming preprotein at the inner membrane translocase TIM23. After insertion into the inner membrane, the soluble, mature protein can be released into the IMS by the inner membrane protease (IMP) (20–22). The second class of IMS proteins possesses characteristic cysteine motifs that typically are either twin CX_9C or twin CX_3C motifs (23, 24). Upon translocation across the outer membrane via the TOM complex, disulfide bonds are formed within the preproteins, which traps them in the IMS. Disulfide bond formation is mediated by the MIA machinery, which consists of the inner-membrane-anchored Mia40 and the soluble IMS protein Erv1 (25–28).

The release of cytochrome *c* from the IMS upon binding and insertion of Bax at the outer membrane is a hallmark of programmed cell death. Although Bax is found only in higher eukaryotes, it was shown that recombinant mammalian Bax induces the release of cytochrome *c* upon incubation with isolated yeast mitochondria (29, 30). Furthermore, we found that not only cytochrome *c* but also other soluble IMS proteins are released from Bax-treated yeast mitochondria, whereas soluble matrix proteins largely remain within the organelle (30).

We used this apparently conserved mechanism to systematically profile the protein composition of the yeast mitochondrial IMS by employing an experimental approach based on stable isotope labeling, which allowed for the specific identification of Bax-dependent protein release. Almost the entire set of known soluble IMS proteins was identified, and 20 additional, novel soluble IMS proteins were found. We confirmed IMS localization for 15 proteins through biochemical assays. Among these proteins, we identified novel proteins that fall into several classes: (i) those that are involved in maintaining protein redox homeostasis (thioredoxins, thioredoxin reductases, or thiol peroxidases), (ii) those that undergo proteolytic processing by IMP (Ptc5), (iii) those that utilize the MIA pathway for their import (Mic23 and Coa6), and (iv) those that play a role in the assembly of cytochrome *c* oxidase (Coa6).

EXPERIMENTAL PROCEDURES

Yeast Strains and Isolation of Mitochondria—The following *Saccharomyces cerevisiae* strains were used: YPH499 (31), BY4741 (Euroscarf, Frankfurt, Germany), BY4741 rho^0 (32), *tom5*Δ (33), *tom22*Δ (34), and *mia40–3* (35). *imp1*Δ, *imp2*Δ, and *coa6*Δ strains were from Euroscarf. Yeast cells were grown at 19 °C, 24 °C, 30 °C, or 33 °C on nonfermentable (1% (w/v) yeast extract, 2% (w/v) bacto peptone, 3% (w/v) glycerol, HCl (pH 5.0)) or fermentable (2% (w/v) sucrose instead of glycerol) medium.

For SILAC analysis, *arg4*Δ cells in the YPH499 background (36) were grown on minimal medium (6.7% (w/v) yeast nitrogen base without amino acids, 2% (w/v) glucose, 0.77% (w/v) Complete Supplement Mixture minus lysine and arginine). Arginine and lysine were added in light ($^{12}C_6$ arginine and $^{12}C_6$ lysine) or heavy forms in two different combinations: either L-arginine HCl U-$^{13}C_6$ and L-lysine U-$^{13}C_6$ or L-arginine HCl U-$^{13}C_6$ U-$^{15}N_4$ and L-lysine 2HCl U$^{13}C_6$ U-$^{15}N_2$. Crude mitochondria were isolated by means of differential centrifugation and further purified via sucrose gradient centrifugation as described elsewhere (37). Growth behavior was assessed by spotting serial dilutions of yeast cells on agar plates with either fermentable or nonfermentable carbon sources, followed by incubation at the indicated temperatures.

Bax-induced Release of IMS Proteins from SILAC-labeled Mitochondria—Mitochondria were incubated in 250 mM sucrose, 150 mM KCl, and 10 mM MOPS-KOH (pH 7.2) in the presence or absence of 100 nM human Bax for 1 h at 37 °C (29, 30). Supernatant and pellet fractions were separated via centrifugation at 20.000 × *g* for 15 min at 4 °C. For the generation of total soluble fractions (SN_{Tot}), mitochondria were resuspended in 250 mM sucrose, 150 mM KCl, and 10 mM MOPS-KOH (pH 7.2) and sonicated five times for 20 s with 40 s breaks. SN_{Tot} fractions were cleared via centrifugation at 100.000 × *g* for 45 min at 4 °C.

In Vitro Import of Preproteins into Isolated Mitochondria—Radiolabeled precursor proteins were synthesized in rabbit reticulocyte lysate system (Promega, Mannheim, Germany) in the presence of [^{35}S]methionine (38). Mitochondria (80 μg) and up to 10% (v/v) radiolabeled precursor protein were incubated in import buffer (10 mM MOPS-KOH (pH 7.2), 3% (w/v) bovine serum albumin (omitted for import of [^{35}S]Trx1 and [^{35}S]Tim9), 250 mM sucrose, 5 mM $MgCl_2$, 80 mM KCl, 5 mM KPi) supplemented with 2 mM ATP and 2 mM NADH for between 5 and 60 min at 30 °C. For dissipation of the membrane potential across the inner mitochondrial membrane, 1 μM valinomycin, 20 μM oligomycin, and 8 μM antimycin A (AVO mix) were added prior to the import reaction. Where indicated, samples were incubated with 50 μg/ml Proteinase K (Prot. K) followed by 10 min incubation with 2 mM phenylmethylsulphonyl fluoride. Mitochondria were reisolated, and washed with SEM buffer (250 mM sucrose, 0.5 mM EDTA, 0.5 M MOPS-KOH (pH 7.2)), and pellets were resuspended in Lämmli buffer following 15 min incubation at 65 °C (38). Samples were analyzed via SDS-PAGE and digital autoradiography (PhosphorImager, Molecular Dynamics, Sunnyvale, CA). For the generation of mitoplasts, mitochondria were swollen in 400 μl EM buffer (0.5 mM EDTA, 0.5 M MOPS-KOH (pH 7.2)) and incubated on ice for 30 min. Samples were treated with Prot. K (50 μg/ml), and mitoplasts were re-isolated via centrifugation at 20.000 × *g* for 15 min at 4 °C (38).

BN-PAGE—For the analysis of native protein complexes, 50 μg mitochondria were solubilized in digitonin buffer (1% (w/v) digitonin, 20 mM Tris-HCl (pH 7.4), 0.5 mM EDTA, 10% (v/v) glycerol, 50 mM NaCl) or dodecylmaltoside (DDM) buffer (0.6% DDM instead of digitonin). A clarifiying spin (20.000 × *g*, 5 min, 4 °C) was performed to remove nonsolubilized mitochondria, and the supernatant was analyzed using BN-PAGE (4% to 13% or 4% to 16.5% gradient gels) followed by immunodecoration (39, 40).

Antisera—Antibodies were generated by immunizing rabbits with synthetic peptides that were coupled to keyhole limpet hemocyanin via N-terminal cysteines. The following peptide sequences were used: Mpm1 (CPQVKHKVVSVDEDN), Pet191 (CREEMEKLKLLNSQQKD), Ptc5 (CVMNPEATTKPKPRL), Cox12 (CEKWDDQRE KGIFAGDINSD), and Nce103 (CEDGLLQTVSTYTKVTPK). Immunodecoration was performed according to standard protocols and developed using ECL™ Western blotting Detection Reagents (GE Healthcare).

MS Sample Preparation—All samples were independently processed and analyzed in two biological replicates, including label-switches and the usage of different heavy amino acid labels leading to four different replicates in total (see above). The protein concentration of mitochondria was determined via Bradford assay and adjusted to 10 mg/ml. Supernatants (SN) from Bax release assays (using 500 μg mitochondria) and total soluble fractions (SN_{Tot}; 500 μg mitochondria) were pooled 1:1 (v/v), resulting in two different samples for each replicate: SN_{Bax}/SN_{Con} (SN BAX-treated *versus* SN non-BAX-treated) and SN_{Bax}/Tot (SN BAX-treated *versus* total soluble fraction). Disulfide bonds were reduced with 10 mM DTT for 30 min at 56 °C, and subsequently free sulfhydryl groups were carbamidomethylated using 30 mM iodoacetamide for 30 min at room temperature in the dark. Prior to digest, samples were diluted 2-fold with 50 mM NH_4HCO_3, and acetonitrile (ACN) and $CaCl_2$ were added to final concentrations of 5% and 1 mM, respectively. Trypsin (protease:protein ratio of 1:30) was added and samples were incubated at 37 °C for 12 h. Peptide samples were cleaned up using Omix C18 tips (Agilent, Waldbronn, Germany) according to the manufacturer's instructions and dried under vacuum. Samples were resuspended in 10 mM KH_2PO_4 (pH 2.7) and further fractionated using strong cation exchange chromatography (SCX).

Strong Cation Exchange Chromatography—SCX was performed using a self-packed 150 mm × 550 μm PolySULFOETHYL A column (200 Å pore size, 5 μm particle size) (PolyLC, Columbia, MD) in combination with an Ultimate 3000 HPLC system (Dionex, Amsterdam, the Netherlands). Peptides were separated at a flow rate of 6 μl/min with a binary gradient (SCX buffer A: 10 mM KH_2PO_4 (pH 2.7); SCX buffer B: 10 mM KH_2PO4, 350 mM KCl, 15% ACN (pH 2.7)) ranging from 1% to 12% B over 10 min, remaining at 12% B for 5 min, and then increasing from 12% to 50% B over 10 min. SN_{Bax}/Tot fractions were crosswise collected as follows, to optimize two-dimensional orthogonality: (1) flow through; (2) 3 to 5 min, 13 to 15 min, and 23 to 25 min; (3) 5 to 7 min, 15 to 17 min, and 25 to 27 min; (4) 7 to 9 min, 17 to 19 min, and 27 to 29 min; (5) 9 to 11 min, 19 to 21 min, and 29 to 31 min; and (6) 11 to 13 min, 21 to 23 min, and 31 to 33 min. SN_{Bax}/SN_{Con} replicates were collected likewise; however, because of the lower sample concentration and complexity, four instead of six pooled samples were generated.

Subsequently, SCX fractions were desalted using Omix C18 tips according to the manufacturer's instructions and dried under vacuum. Samples were resuspended in 0.1% TFA and further analyzed via LC-MS.

LC-MS Analysis—Nano-LC-MS/MS was performed on an LTQ-Orbitrap Velos mass spectrometer (Thermo Fisher Scientific, Bremen, Germany) coupled to an Ultimate 3000 Rapid Separation Liquid Chromatography system (Dionex, Germering, Germany). Briefly, peptides were preconcentrated on a C18 trapping column (Acclaim PepMap, 100 μm × 2 cm, 5 μm particle size, 100 Å pore size, Dionex) in 0.1% TFA and separated on a C18 main column (Acclaim PepMap, 75 μm × 25 cm, 2 μm particle size, 100 Å pore size, Dionex) using a binary gradient (solvent A: 0.1% formic acid (FA); solvent B: 0.1% FA, 84% ACN) ranging from 5% to 45% B over 240 min, at a flow rate of 300 nl/min.

MS survey scans were acquired in the Orbitrap from 300 to 2000 *m/z* at a resolution of 60,000 using the polysiloxane *m/z* 371.101236 as a lock mass (41). The ten most intense signals above charge state +1 were subjected to collision induced dissociation (CID) in the ion trap, taking into account a dynamic exclusion of 12 s. CID spectra were acquired with a normalized CE of 35%, a default charge state of 2, and an activation time of 30 ms. Automatic gain control target values were set to 10^4 for ion trap MS^n and 10^6 for Orbitrap MS scans.

Data Interpretation—Data interpretation was accomplished with the help of Proteome Discoverer (PD) 1.3 (Thermo Scientific). Data were searched with Mascot 2.3 (Matrix Science, London, UK) (42) and Sequest (43) against the Saccharomyces Genome Database (January 5, 2010; 6717 sequences) using the following settings: (1) trypsin without any missed cleavage sites; (2) carbamidomethylation of cysteine as fixed; (3) depending on the utilized heavy amino acids for SILAC labeling, either $^{13}C_6$ Lys and $^{13}C_6$ Arg (both +6.02 Da) or $^{13}C_6{}^{15}N_2$ Lys (+8.01 Da) and $^{13}C_6{}^{15}N_4$ Arg (+10.01 Da) as variable modifications; and (4) MS and MS/MS tolerances of 10 ppm and 0.5 Da, respectively (supplemental Table S4). For quantification only unique peptides were taken into account, and the maximum fold-change was set to 100 in case of missing SILAC doublets.

After the database search, the following filter criteria were applied to all results: (1) high confidence corresponding to a false discovery rate (FDR) < 1%, (2) maximum peptide rank 1, (3) minimum Mascot score > 20, and (4) minimum XCorr 2.0, 2.5, 2.5, and 2.75 for charge states +2, +3, +4, and +5.

SILAC protein ratios were calculated by PD based on peptides for which both channels (heavy and light) or only a single channel (heavy or light) could be quantified. In the latter case, artificial ratios might increase quantification variability. Protein ratios based on single peptides were manually validated in the raw data (see supplemental Table S3 and supplemental Fig. S1). Still, for discrete candidate proteins, SILAC ratios could not be determined for all biological replicates and all different IMS samples. To compensate for those missing SILAC ratios, additional data interpretation was conducted using PeptideShaker version 0.12.0 (http://code.google.com/p/peptide-shaker/) in order to identify missing candidate peptides based on multi-search engine database searches, including Mascot, OMSSA (44), and X!Tandem (45), combined with a thorough FDR assessment (46). Therefore, raw data were converted to the Mascot generic format using Proteowizard software (version 2.1) (47) and database searches were conducted using SearchGUI-1.6.5 (48) and Mascot 2.3. Indeed, one missing candidate peptide (supplemental Table S3; supplemental Fig. S1) could be detected within the final 1% FDR (protein level) results list, and *m/z* value and retention time were used to manually determine the SILAC ratios based on monoisotopic MS signal intensities in the raw data using Xcalibur Qual Browser 2.1 (supplemental Table S3). A comprehensive list of all reproducibly identified proteins, including their SN_{Bax}/SN_{Con} and SN_{Bax}/Tot ratios, is available in supplemental Table S5.

RESULTS

Profiling of Protein Release from Bax-stimulated Mitochondria—In order to profile the specific release of soluble IMS proteins upon Bax-induction, we purified mitochondria from yeast strains grown in the presence of isotope-labeled ("heavy") or nonlabeled ("light") amino acids (Fig. 1). The obtained highly pure mitochondria were incubated in the presence or absence of Bax, and protein release was monitored by immunodecoration of both SN and the remaining mitochondrial pellet fractions. IMS proteins like cytochrome *c* or the soluble isoform of Mcr1 were largely released into the SN, whereas most of the matrix proteins, like Aco1 or Cit1, remained in the pellet (Fig. 1*A*). However, we noticed that a minor fraction of some matrix proteins (*e.g.* Aco1) was released upon Bax treatment as well, and other matrix proteins (*e.g.* Cit1) were detected in tiny amounts in the SN independently of Bax (Fig. 1*A*). Thus, a simple comparison of peptide ratios in the SN from Bax-treated and nontreated mitochondria identified via MS could easily lead to false positive hits.

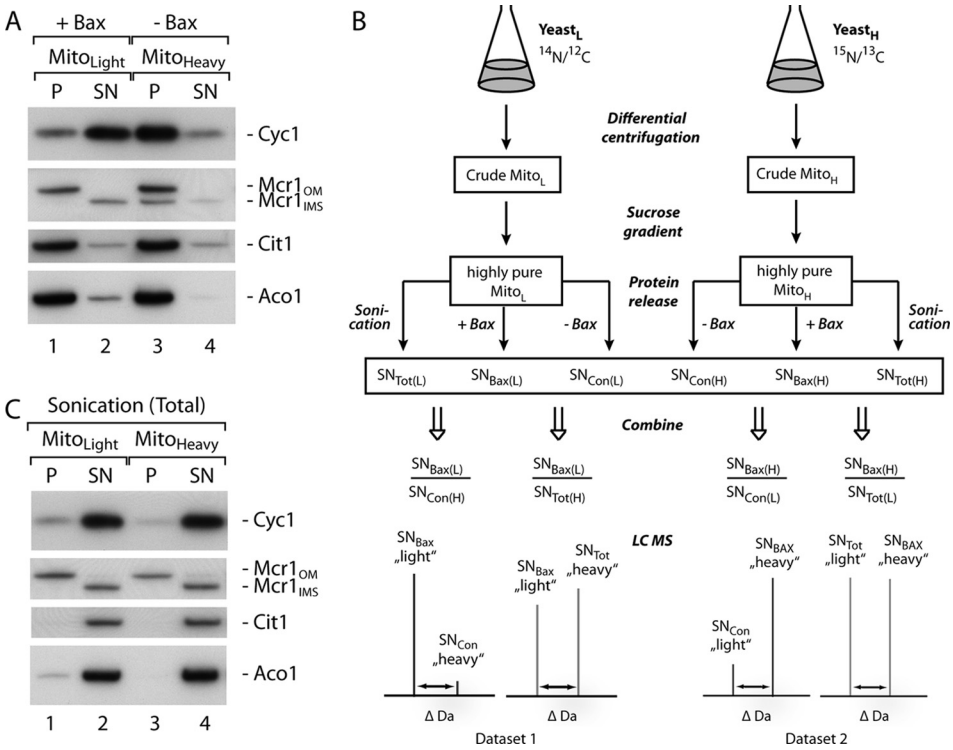

FIG. 1. **Experimental approach to profile mitochondrial IMS proteins upon Bax-induced release.** *A*, Mitochondria were isolated from wild-type yeast cells grown on either "light" or "heavy" amino acids (Arg, Lys) and incubated in the presence or absence of 100 nM Bax for 1 h at 37 °C. Pellet (P) and supernatant (SN) fractions were separated via centrifugation and analyzed by means of SDS-PAGE followed by immunoblotting. *B*, Schematic overview of experimental strategy. *C*, Isolated mitochondria from yeast cells labeled with either light or heavy amino acids were subjected to sonication followed by centrifugation to yield total soluble mitochondrial proteins (SN).

We therefore employed a strategy comparing the amount of released protein to its total amount present in soluble whole mitochondrial extracts (Fig. 1*B*). In the case of IMS proteins, we would expect that the major part of the protein would be released, whereas in contrast matrix proteins should be present in the SN only in small amounts. Soluble extracts from whole mitochondria were generated by sonication and cleared of membrane fractions by a consecutive centrifugation step. Immunodecoration revealed that soluble mitochondrial proteins from both matrix and IMS were quantitatively extracted (Fig.1*C*).

We generated two independent sets of isotope-labeled and highly purified mitochondria. For each set ($Mito_{Heavy}$ and $Mito_{Light}$), we performed the Bax treatment twice, and $Mito_{Heavy}$ and $Mito_{Light}$ were switched once to ensure an unbiased profiling (Fig. 1*B*). This resulted in four different sets of samples (1–4). We measured the peptide ratios for each set, including SN after Bax release compared with control release without the addition of Bax (SN_{Bax}/SN_{Con}) and SN after Bax release compared with the total soluble fraction (SN_{Bax}/Tot).

Each set of samples was combined, carbamidomethylated, and digested using trypsin. To reduce sample complexity, samples SN_{Bax}/Tot and SN_{Bax}/SN_{Con} were separated via SCX into six and four fractions, respectively, which were desalted by means of C18 solid-phase extraction and analyzed via nano-LC-MS. For each individual sample set, raw files of all fractions were processed batch-wise using PD. Respective SILAC ratios, which were quantified by single spectra, were manually validated in the raw data (supplemental Fig. S1); all data are summarized in supplemental Table S3. For some proteins, quantitative data were missing for certain replicates, so we conducted an additional database search using the software PeptideShaker, which combines three search algorithms (Mascot, OMSSA, and X!Tandem), to identify additional peptides for quantification. Heavy/light ratios for the corresponding spectra were subsequently determined manually within the raw data based on the intensities of monoisotopic signals and are labeled in supplemental Table S3.

We first filtered identified proteins and their peptide ratios that were reproducibly found in at least three of the four datasets for their annotation as IMS proteins in the yeast genome database (49). We identified 29 of 31 known IMS proteins that have been described as soluble or only loosely bound to the inner membrane (49) (supplemental Table S1). All proteins revealed the expected high SN_{Bax}/SN_{Con} values (on average, a 20-fold increase after Bax induction) and SN_{Bax}/Tot values close to 1 (0.74 on average), meaning that a major fraction of these proteins is specifically released from mitochondria upon Bax treatment. We then analyzed peptide ratios for 59 proteins that had been reproducibly identified

and which are annotated as matrix proteins (supplemental Table S2). For some of these matrix proteins we observed a Bax-dependent release as well; however, the mean SN_{Bax}/SN_{Con} value of 2.5 (for all 59 matrix proteins) is significantly lower than that for the known IMS proteins. Next we searched for novel proteins that revealed SN_{Bax}/SN_{Con} values of at least 7 and SN_{Bax}/Tot values of at least 0.5. Twenty proteins fulfilled these criteria and therefore represent candidates for novel IMS proteins (Table I and supplemental Table S3). Ten of these proteins have not been localized to mitochondria yet, and the other proteins were either found in proteomic studies of purified mitochondria (1, 50) or annotated as inner membrane proteins (Table I). Three proteins encoded by the open reading frames—Ybl107c, Ybr056w, and Ymr244c-a—represent novel mitochondrial proteins of unknown function.

Validation of Novel IMS Protein Candidates—To validate IMS localization of the identified candidate proteins, we employed various biochemical techniques, including Bax-release assays with specific antibodies, *in organello* import of radiolabeled preproteins, and protease accessibility to the IMS upon osmotic swelling. Specific antisera were generated for five proteins: Mpm1 (mitochondrial peculiar membrane protein), Pet191 (PETite colonies), Ptc5 (phosphatase two C), Cox12 (subunit VIb of cytochrome *c* oxidase), and Nce103 (nonclassical export). For Qcr6 (subunit 6 of the ubiquinol cytochrome *c* reductase complex), a specific antibody was available (51). We incubated isolated mitochondria with and without Bax and tested for the specific release of IMS proteins through immunoblotting. We found a specific (Bax-dependent) release of cytochrome *c* and the IMS form of Mcr1, whereas proteins from other mitochondrial compartments remained largely unaffected (Fig. 2*A*, lanes 2 and 4). The same samples were then tested for the novel IMS candidate proteins Mpm1, Pet191, Cox12, Ptc5, and Qcr6. All proteins were specifically and efficiently released from mitochondria upon Bax treatment (Fig. 2*A*, lanes 6 and 8), demonstrating their localization in the IMS. For Ptc5 and Qcr6, we observed that approximately half of the protein amount was still present in mitochondria after Bax-release, indicating that a fraction of these proteins is still tightly associated with the inner membrane. Indeed, for Qcr6 this is quite likely, as it was found as a stoichiometric component of the cytochrome *bc1* complex (12, 52). However, our results revealed that a significant fraction of Qcr6 was in a soluble or releasable state. To further validate the IMS localization of these candidate proteins, we tested for their accessibility to externally added protease upon rupture of the outer membrane. Mitochondria and mitoplasts that were generated by osmotic swelling were treated with and without Prot. K. Immunoblotting showed that the outer membrane protein Tom70 was digested by Prot. K in mitochondria and mitoplasts, whereas the IMS-exposed domain of the inner membrane protein Tim50 is only accessible to Prot. K in mitoplasts (Fig. 2*B*, lanes 2 and 4). The matrix proteins Pam17 and Mge1 remained unaffected under both conditions. We then tested these samples for the novel IMS candidate proteins Mpm1, Cox12, Nce103, Pet191, and Qcr6 and found that all were protected in mitochondria but became accessible to Prot. K upon rupture of the outer membrane (Fig. 2*B*, lanes 6 and 8), demonstrating their localization in the IMS. The levels of some proteins (*e.g.* Nce103) were already decreased in mitoplasts without Prot. K treatment, reflecting an efficient release from the IMS upon osmotic swelling.

In a further set of experiments we validated the sublocalization of IMS candidate proteins via *in organello* import of radiolabeled preproteins into isolated mitochondria. Preproteins were generated by *in vitro* transcription/translation in the presence of [^{35}S]methionine (38) and incubated with mitochondria in the presence or absence of the membrane potential $\Delta\psi$, which was depleted via the addition of valinomycin prior to the import reaction. Most proteins localized to the IMS do not require the membrane potential for their import, and typically no processing of a presequence is observed (38); for example, the IMS model substrate [^{35}S]Tim9 is imported into a Prot. K protected location independently of $\Delta\psi$ (Fig. 3*A*, lanes 4 and 5) (27, 35, 38). Unlike Tim9, the matrix targeted preprotein [^{35}S]Mdh1 shows a $\Delta\psi$-dependent processing to its mature form upon import (Fig. 3*A*, lanes 4 and 5). We generated radiolabeled preproteins for 11 novel IMS candidate proteins and tested their import into isolated mitochondria. For 10 proteins the import profile was similar to that of [^{35}S]Tim9 (*i.e.* Prot. K protection, no $\Delta\psi$-dependence, and no presequence processing) (Fig. 3*A*), indicating import into the IMS. For [^{35}S]Ptc5, however, we observed membrane-potential-dependent processing of the preprotein (Fig. 3*A*, lanes 9 and 10, top panel), which suggests that the import route of Ptc5 into the IMS could involve the presequence import pathway and processing by IMP. For the IMS candidate proteins that revealed an import profile similar to that of Tim9, we additionally tested sublocalization of radiolabeled preproteins after import by Prot. K accessibility upon osmotic swelling as described above. We found that all novel IMS candidate proteins are, like Tim9, accessible to Prot. K in mitoplasts but protected in mitochondria. In contrast, the matrix protein Mdh1 remained protected upon swelling (Fig. 3*B*, lanes 5–6 and 8–9).

With these data taken together, we could biochemically validate the IMS localization for 15 proteins that were identified by our differential proteomics approach. The remaining five candidate proteins could not be tested because of a lack of specific antibodies and the inefficient generation of radiolabeled preproteins.

The Protein Phosphatase Ptc5 is a Novel Substrate of the Inner Membrane Protease IMP—The protein phosphatase Ptc5 has been identified in the mitochondrial proteome and is suggested to be involved in the regulation of the pyruvate dehydrogenase (PDH) complex (50, 53). PDH activity is decreased in *ptc5*Δ mitochondria, and Ptc5 was found to comi-

TABLE I

List of novel proteins that are specifically and efficiently released from yeast mitochondria upon Bax treatment

ORF	Gene name	Gene annotation	Localization[a]	Molecular weight (kDa)	Sequence coverage (%)	Twin C(X)$_n$C motif	SN_{BAX}/SN_{Con}[b]	SN_{BAX}/Tot[b]	IMS localization confirmed biochemically (this study)
YBL107C	**YBL107C**	Putative protein of unknown function	Cytosol	23.0	55.1	$CX_{14}C$, $CX_{13}C$	33.9	0.8	Yes
YDR155C	**CPR1**	Cytoplasmic peptidyl-prolyl cis-trans isomerase	Cytosol, mitochondria	17.4	41.4		8.2	0.9	Yes
YDR353W	**TRR1**	Cytoplasmic thioredoxin reductase	Cytosol	34.2	42.0		19.7	0.6	Yes
YER057C	**HMF1**	Member of the p14.5 protein family	Cytosol, nucleus	13.9	57.4		20.1	0.5	Yes
YFR033C	**QCR6**	Subunit 6 of the ubiquinol cytochrome-c reductase complex	Integral to IM	17.3	32.0		29.8	0.5	Yes
YIR037W	**HYR1**	Thiol peroxidase	Intracellular	18.6	41.1		7.3	0.6	Yes
YJL066C	**MPM1**	Mitochondrial membrane protein of unknown function	Mitochondrial membrane	28.5	65.9		24.6	0.5	Yes
YJR034W	**PET191**	Protein required for assembly of cytochrome c oxidase	Integral to IM	12.4	57.4	Twin CX_9C	9.3	0.7	Yes
YKL152C	**GPM1**	Tetrameric phosphoglycerate mutase	Cytosol, mitochondria	27.6	65.9		45.4	0.7	Yes
YLR038C	**COX12**	Subunit VIB of cytochrome c oxidase	Integral to IM	9.8	79.5	CX_9C, $CX_{10}C$	14.9	0.7	Yes
YLR043C	**TRX1**	Cytoplasmic thioredoxin	Cytosol	11.2	54.4		29.0	0.9	Yes
YMR244C-A	**YMR244C-A**	Putative protein of unknown function	Cytosol, nucleus	12.4	32.7	CX_9C, $CX_{10}C$	7.8	0.7	Yes
YNL036W	**NCE103**	Carbonic anhydrase	Cytosol, nucleus	24.9	19.9	Twin CX_8C	14.4	0.6	Yes
YOL143C	**RIB4**	Lumazine synthase	Cytosol, nucleus	18.6	26.0		52.3	0.8	Yes
YOR090C	**PTC5**	Mitochondrial type 2C protein phosphatase	Mitochondria	63.7	35.1		14.6	0.6	Yes
YBR035C	**PDX3**	Pyridoxine phosphate oxidase	Unknown	26.9	25.0		20.0	0.6	
YBR056W	**YBR056W**	Putative protein of unknown function	Cytosol	57.8	6.6		7.0	0.6	
YIL160C	**POT1**	3-ketoacyl-CoA thiolase	Peroxisome	44.7	38.4		7.0	0.6	
YPL132W	**COX11**	Protein required for delivery of copper to Cox1 subunit	Integral to IM	34.0	16.3		24.4	0.8	
YMR228W	**MTF1**	Mitochondrial RNA polymerase specificity factor	Mitochondria	39.7	10.6		11.8	1.0	

[a] Annotated localization in the Saccharomyces Genome Database (49).

[b] SN_{BAX}/SN_{Con} and SN_{BAX}/Tot are averaged peptide ratios from four different replicates (see supplemental Table S3).

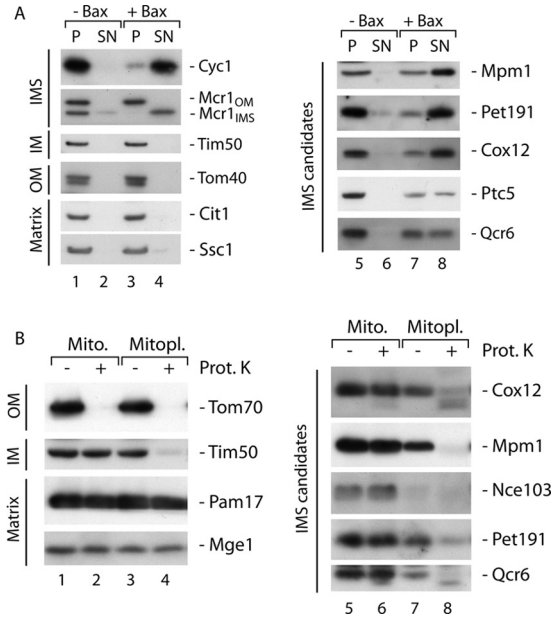

FIG. 2. **Sublocalization of novel IMS proteins.** *A*, Release of novel IMS proteins from mitochondria upon Bax treatment. Mitochondria were incubated in the presence or absence of 100 nM Bax for 1 h at 37 °C. Pellet (P) and supernatant (SN) were separated via centrifugation, and the samples were analyzed by means of SDS-PAGE followed by immunoblotting. *B*, Protease accessibility of novel IMS proteins upon osmotic swelling. Mitoplasts were generated via the treatment of mitochondria in hypotonic buffer. Where indicated, mitochondria (Mito.) and mitoplasts (Mitopl.) were subsequently treated with Prot. K. Samples were analyzed via SDS-PAGE and immunoblotting.

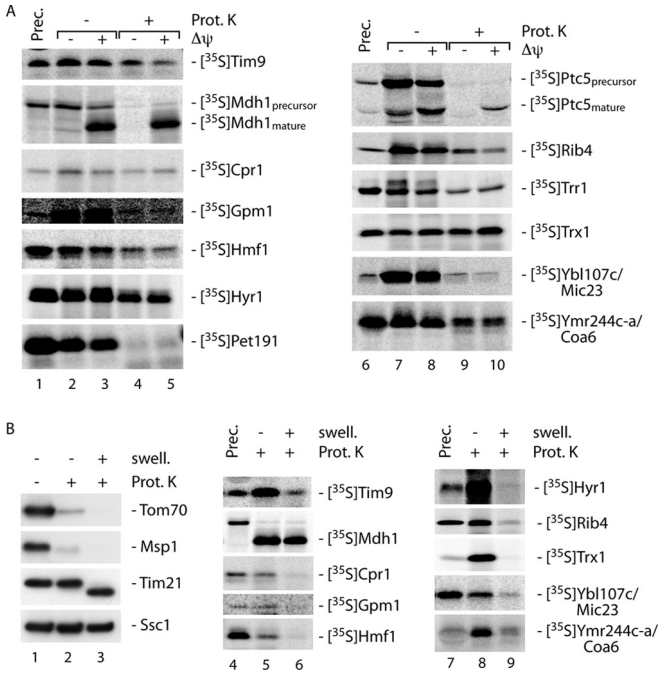

FIG. 3. **Import of radiolabeled IMS precursor proteins into isolated mitochondria.** *A*, Isolated mitochondria were incubated with ^{35}S-labeled precursor proteins. Where indicated, the membrane potential was dissipated prior to the import reaction, and samples were treated with Prot. K. Samples were analyzed via SDS-PAGE and autoradiography. *B*, ^{35}S-labeled precursor proteins were imported into isolated mitochondria, followed by treatment in hypotonic buffer (+ swell.) and digestion with Prot. K where indicated. Samples were separated by means of SDS-PAGE followed by immunoblotting (as control for Prot. K treatment and swelling; lanes 1–3) and autoradiography (lanes 4–9).

grate with the PDH complex on blue native PAGE (53). It was therefore proposed to interact with the PDH complex in the mitochondrial matrix. We found Ptc5 to be a novel IMS candidate protein that is specifically released upon Bax treatment (Fig. 2*A*). However, *in organello* import of [^{35}S]Ptc5 revealed the involvement of the presequence import pathway (Fig. 3*A*). This might indicate that Ptc5 is indeed a matrix protein or that it is released into the IMS upon arrest at the presequence import machinery and cleavage by IMP (20–22). When we tested for Ptc5 in mitochondria and mitoplasts by immunoblotting, a large fraction of the protein was released upon osmotic swelling, and a further fraction was accessible to Prot. K, indicating IMS localization (Fig. 4*A*, lanes 3 and 4). We tested further to see whether Ptc5 is a substrate of IMP consisting of the two catalytic subunits Imp1 and Imp2 (20–22). Immunoblotting of mitochondria from wild-type and *imp1*Δ strains revealed a larger form of Ptc5 that might represent an intermediate generated upon processing by the matrix processing peptidase that cannot be further processed to the mature form because of the lack of Imp1 (Fig. 4*B*). To test this, we imported [^{35}S]Ptc5 into wild-type and *imp1*Δ mitochondria. Indeed, imported Ptc5 accumulated in the intermediate form in *imp1*Δ mitochondria, but it was further processed in wild-type mitochondria (Fig. 4*C*, lanes 3 and 4). Processing of [^{35}S]Ptc5 preprotein in *imp2*Δ mitochondria was not affected (Fig. 4*C*, lanes 8 and 9). Our results show that Ptc5 represents a novel IMS protein that is imported via the presequence pathway followed by IMP processing, releasing the soluble protein into the IMS.

Identification of Novel Substrates of the MIA Import Machinery—A subset of IMS proteins is imported via the MIA machinery, the main components of which, Mia40 and Erv1, provide an oxidoreductase system (8, 18, 19, 25, 26, 54). The MIA machinery facilitates the formation of disulfide bonds within preproteins after their passage across the outer membrane, thereby trapping the proteins in the IMS (16, 25, 35, 55). MIA-dependent preproteins contain characteristic cysteine motifs. These are typically twin (CX_9C) or twin (CX_3C) motifs (8, 23, 24, 35). In order to identify novel MIA substrates, we inspected our list of novel IMS candidate proteins for the presence of these characteristic cysteine motifs. Only for Pet191 was a typical twin (CX_9C) motif found. However, we noticed that some proteins possessed unusual twin (CX_nC) motifs: Cox12 and Ymr244c-a have single (CX_9C) and ($CX_{10}C$) motifs, and Nce103 and Ybl107c possess twin (CX_8C) or single ($CX_{14}C$) and ($CX_{13}C$) motifs, respectively (Table I). We

wondered whether import of these proteins requires the MIA machinery. We employed the temperature-sensitive mutant *mia40–3*, which is impaired in the import of IMS proteins with twin (CX_9C) and twin (CX_3C) motifs (23, 35). This can be shown by a reduced protein level in mutant mitochondria or an impaired rate of preprotein import *in organello* (23, 35). We tested the protein levels of Cox12 and Pet191 in wild-type and *mia40–3* mitochondria by immunoblotting and found a significant reduction of both proteins in the mutant mitochondria relative to the wild-type (Fig. 5*A*). The levels of other mitochondrial proteins that are MIA-independent remained unchanged (Fig. 5*A*).

The proteins Ybl107c and Ymr244c-a were further analyzed via import of the radiolabeled preproteins into isolated mitochondria. We first asked whether import of both preproteins requires the TOM complex for transport across the outer membrane. This was assayed using mitochondria lacking Tom5 or Tom22, respectively. Tom22 functions as a central preprotein receptor (34). In addition, Tom5 was found to play a role in the biogenesis of small Tim proteins (33, 56). Import of [^{35}S]Tim9 and [^{35}S]Mdh1 is significantly impaired in *tom5*Δ and *tom22*Δ mitochondria, respectively (Figs. 5*B* and 5*C*). Both preproteins Ybl107c and Ymr244c-a showed a decreased import rate in *tom5*Δ and *tom22*Δ mitochondria (Figs. 5*B* and 5*C*), demonstrating that they are imported into mitochondria via the central protein entry gate TOM. Compared with wild-type, the import into *mia40–3* mitochondria was also significantly impaired, similarly with regard to the import of [^{35}S]Tim9 that contains the classical twin CX_9C motif. Import of the matrix targeted [^{35}S]Mdh1 remained unchanged (Fig. 5*D*).

Our results demonstrate the requirement of the MIA import machinery for Pet191, Cox12, Ybl107c, and Ymr244c-a, of which three contain unusual cystein motifs. We termed the open reading frame Ybl107c Mic23 (for *mitochondrial intermembrane space cysteine motif protein of 23 kDa*). The pro-

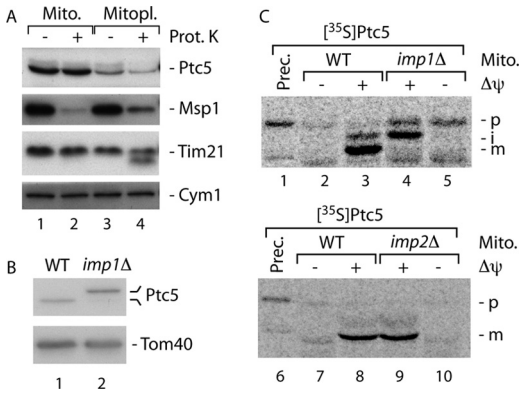

FIG. 4. **Ptc5 is a novel substrate of the presequence/IMP import pathway into the IMS.** *A*, Mitochondria were incubated in isotonic (lanes 1 and 2) or hypotonic (lanes 3 and 4) buffer, followed by digestion with Prot. K where indicated. Analysis was performed via SDS-PAGE and immunoblotting. Mito., mitochondria; Mitopl., mitoplasts; Mat., matrix. *B*, Western blot analysis of mitochondria isolated from wild-type (WT) or *imp1*Δ strains. *C*, ^{35}S-labeled precursor of Ptc5 was incubated with wild-type (WT), *imp1*Δ, or *imp2*Δ mitochondria, followed by treatment with Prot. K. Where indicated, the membrane potential (Δψ) was dissipated prior to the import reaction. Samples were analyzed via SDS-PAGE and autoradiography. Prec., precursor; i, intermediate; m, mature protein.

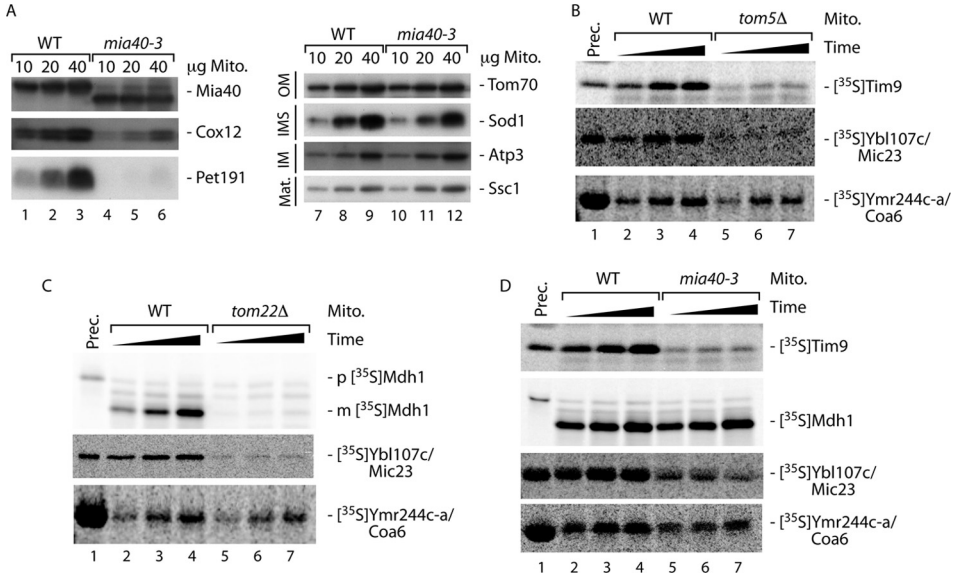

FIG. 5. **Novel substrates of the MIA import machinery.** *A*, Mitochondria isolated from wild-type (WT) and *mia40–3* yeast cells were analyzed via SDS-PAGE and immunoblotting. *B*, Radiolabeled precursor proteins were imported into wild-type (WT) and *tom5*Δ mitochondria for increasing periods of time. Samples were treated with Prot. K and analyzed via SDS-PAGE and autoradiography. Prec., precursor. *C,* WT and *tom22*Δ mitochondria were incubated with ^{35}S-labeled preproteins, followed by treatment with Prot. K and analysis via SDS-PAGE and autoradiography. *D*, Radiolabeled preproteins were incubated with WT or *mia40–3* mitochondria. Samples were subsequently treated with Prot. K and analyzed via SDS-PAGE and autoradiography. Prec., precursor.

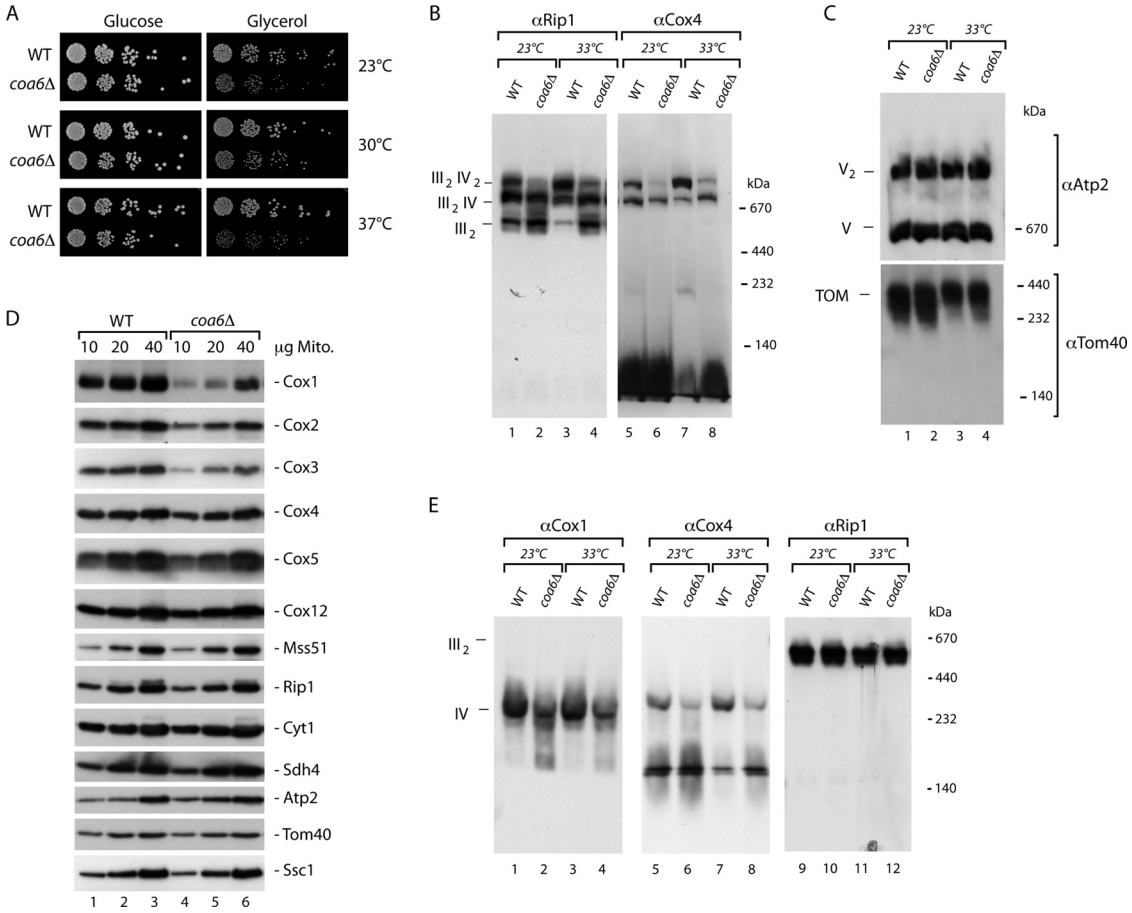

FIG. 6. **The novel IMS protein Coa6 is required for assembly of cytochrome *c* oxidase.** *A*, Growth of serial dilutions of wild-type (WT) and *coa6*Δ yeast cells on fermentable (YPD) or non-fermentable (YPG) carbon sources at indicated temperatures. *B*, *C*, WT and *coa6*Δ mitochondria isolated after cell growth at either 23 °C or 33 °C were solubilized in digitonin buffer and analyzed via blue native (BN) electrophoresis and immunoblotting. III_2, dimer of respiratory chain complex III; IV, respiratory chain complex IV; TOM, preprotein translocase of the mitochondrial outer membrane; V_2, dimer of ATPase (complex V of respiratory chain). *D*, Western blot analysis of various protein levels of mitochondria from WT or *coa6*Δ cells. *E*, Mitochondria from WT and *coa6*Δ yeast cells grown at either 23 °C or 33 °C were lysed in dodecylmaltoside buffer and analyzed via BN-PAGE and immunodecoration.

tein Ymr244c-a was termed Coa6 for reasons described below.

Coa6 Plays a Role in Assembly of Cytochrome c Oxidase Complex—When we analyzed the growth of a *coa6* deletion strain, we found a severe growth defect of *coa6*Δ cells compared with wild-type under respiratory (glycerol) but not fermentative (glucose) growth conditions (Fig. 6*A*). This respiratory growth defect was observed at all temperatures and indicated a potential role of Coa6 in mitochondrial respiration. We asked whether the absence of Coa6 could affect the organization of respiratory chain complexes. This can be monitored by means of blue native (BN)-PAGE, which can resolve various supercomplex species that contain cytochrome *c* oxidase (complex IV) together with cytochrome *c* reductase (complex III) (39). In yeast, complex IV associates with complex III to form two main supercomplexes that contain dimers of complex III together with either one or two units of complex IV (39, 40, 57, 58). Mitochondria from wild-type and *coa6*Δ cells were solubilized in digitonin buffer and separated via BN-PAGE. Respiratory complexes III and IV were analyzed by immunodecoration with antibodies recognizing the rieske iron-sulfur protein (Rip1) of complex III and Cox4 of complex IV, respectively. We found that the formation of the largest supercomplex, consisting of two dimers of each complex (III_2IV_2), was severely impaired in the absence of Coa6 (Fig. 6*B*), whereas other high molecular weight complexes such as ATP-synthase (complex V) or the TOM complex of the outer membrane remained unchanged (Fig. 6*C*). Furthermore, we observed increased levels of complex III dimers (III_2), which are apparently caused by impaired formation of the III_2IV_2 supercomplex (Fig. 6*B*). We wondered whether Coa6 could play a specific role in the formation of supercomplexes between complexes III and IV, or whether it is required for the assembly of one of the two complexes. When we compared the steady state protein levels of various components of respiratory complexes in wild-type and *coa6*Δ mitochondria, we

found a decrease in the mitochondrial encoded subunits of complex IV (Cox1, Cox2, and Cox3) in the absence of Coa6, whereas other proteins, such as Rip1 and Cyt1 of complex III and nuclear encoded subunits of complex IV, as well as further control proteins, were not changed (Fig. 6*D*). We then analyzed the complexes again via BN-PAGE but solubilized mitochondria with DDM instead of digitonin. DDM leads to the dissociation of respiratory supercomplexes and allows the detection of monomeric complex IV and the dimer of complex III (39, 40). As shown in Fig. 6*E*, we observed significantly lower amounts of complex IV, whereas the levels of complex III dimers remained unchanged.

With these findings taken together, we show that the novel IMS protein Coa6 plays a role in the assembly of cytochrome *c* oxidase and is required for the efficient formation of respiratory supercomplexes. Therefore, we have termed this protein Coa6 (*cytochrome c oxidase assembly factor 6*).

DISCUSSION

So far submitochondrial proteomes have been obtained only from purified outer membranes (4–6). Previous attempts to profile the protein composition of the IMS uncovered only very few proteins or identified many contaminating matrix proteins (59, 60). We present here the first comprehensive analysis of mitochondrial IMS proteins employing a differential proteomics approach. Our strategy to combine the specific and efficient protein release from yeast mitochondria upon Bax stimulation with stable isotope-labeling led to the identification of altogether 49 different proteins with a coverage of >90%. From the 31 known IMS proteins that were described as soluble or only loosely attached to the inner membrane, only two were not identified in this study. These are Rib3, an enzyme of the riboflavin biosynthetic pathway, which has been shown to possess an additional function in mitochondrial respiration (61), and Ups2, which is involved in lipid metabolism (62, 63). Of the 20 novel IMS proteins, 10 had not been localized to mitochondria before. The other proteins were found in global proteomic studies of purified mitochondria or assigned to other submitochondrial compartments (49) (Table I). We validated IMS localization biochemically for 15 candidate proteins, and in each case we found the protein indeed was present in the IMS.

A surprising finding was the efficient Bax-dependent release of Qcr6 and Cox12, which have been described as components of the respiratory chain complexes III and IV in the inner membrane, respectively (52, 64, 65). This might indicate that these proteins are only loosely attached to the complexes and efficiently released by Bax treatment or that they are present in an additional, soluble pool in the IMS and possibly are involved in other functions. Cox12 has been described as playing a role in the assembly of complex IV, but it does not seem to be required for its function, although it has been described as a component of the mature complex (40, 64). These observations point to the possibility that some of the novel IMS proteins identified here are not entirely soluble proteins and could be loosely attached to the inner membrane. It is therefore a matter of definition to classify a protein as an IMS protein. The successful and comprehensive identification of almost all known IMS proteins upon Bax stimulation in this study offers a novel and reliable procedure to define and classify proteins as IMS proteins. In addition, the technique developed for this study offers the possibility of profiling mitochondrial IMS proteins from yeast cells grown under different metabolic conditions and analyzing the IMS proteome from other organisms as well. Especially in mammals, in which the Bax induced release of IMS proteins is of physiological importance, this could lead to the identification of novel players involved in programmed cell death.

Upon biogenesis, precursor proteins destined for the IMS need to be specifically sorted into this submitochondrial compartment. So far, two main import mechanisms have been described. Precursor proteins from one class are imported via the presequence pathway followed by arrest in the inner membrane and release into the IMS upon proteolytic cleavage by IMP (21). However, so far only three proteins of the IMS (Gut2, Cyb2, and Mcr1) have been shown to take this import route in yeast mitochondria (21)—with the protein phosphatase Ptc5 we have identified a novel substrate of this pathway. Considering the 51 proteins in total that are located in the IMS, it is now obvious that the presequence/IMP pathway plays only a minor role in IMS biogenesis. The second protein import route into the IMS requires the MIA machinery, and one dozen substrates have been identified so far (8, 16, 23, 25, 35). It was assumed that MIA-dependent precursor proteins contain twin (CX_9C) or twin (CX_3C) motifs. We have identified four novel MIA-dependent proteins. However, only Pet191, which has been described as an inner membrane protein (66), possesses a classical twin (CX_9C) motif; Cox12 and Coa6 contain a (CX_9C) ($CX_{10}C$) motif, and Mic23 contains a ($CX_{13}C$) ($CX_{14}C$) motif. This might indicate that MIA-dependent precursor proteins possess a much broader range of cysteine motifs than assumed. Alternatively, it is also possible that not all MIA-dependent substrates require a characteristic cysteine motif for their import.

Notably, the majority of IMS proteins are not imported by the presequence/IMP pathway, nor do they contain classical MIA cysteine motifs. It therefore remains open how these proteins are imported into the IMS and whether novel import mechanisms are to be uncovered. Further mechanistic studies will be required to answer these questions, and the proteins identified in our study will provide a highly valuable pool of novel substrates to test.

Many of the novel IMS proteins identified in this study were annotated to be localized to other cellular compartments, for example, the cytosol (Table I). Some of these proteins were sublocalized in high-throughput studies using tags such as GFP (67, 68). Import of these fusion proteins into mitochondria functions quite well for matrix and inner membrane pro-

teins because here a strong import force provided by the inner membrane potential and ATP hydrolysis at the matrix import motor PAM facilitates unfolding of the translocating preprotein, even when it is carrying a cargo such as GFP (14, 18, 19). IMS proteins are imported without these energy sources, and therefore fusion proteins could be mistargeted as a result of an impaired unfolding capacitiy. In the yeast GFP fusion localization database (68), many of the known IMS proteins either were localized to the cytosol and/or the nucleus (*e.g.* Mic14, Mic17, Cox17, Adk1, Cyc1, Mdm35, Sod1, Ynk1, Cox19, Cox23) or were not localized at all (*e.g.* Tim9, Tim10, Tim8, Tim13, Cyb2). Our approach allowed the identification of authentic IMS proteins without fusion tags that could interfere with protein import and IMS sorting. Nevertheless, some proteins are likely dually localized between cytosol and mitochondrial IMS, including the cytoplasmic thioredoxin Trx1, the thioredoxin reductase Trr1, and the peptidyl-prolyl cis-trans isomerase Cpr1 (69, 70). So far only the superoxide dismutase Sod1 has been dually localized in the IMS and the cytosol (8). Further studies need to clarify which mechanisms regulate such a dual localization. For Trx1 and Trr1, it will be also interesting to analyze their role in redox regulation in the IMS. It is possible that they are involved in preventing unwanted disulfide bond formation of IMS proteins and that they could function together with the MIA machinery.

A further interesting novel IMS protein is Rib4, which is involved in riboflavin biosynthesis (71). Rib4 could have a different role in the IMS that is similar to that of its related protein Rib3, which is (in addition to its function in riboflavin synthesis) also involved in mitochondrial respiration (61). Alternatively, the presence of both proteins (Rib3 and Rib4) in the IMS could also indicate a direct link between riboflavin biosynthesis and respiration.

So far Coa6 has not been localized to a cellular compartment and has been annotated as an open reading frame (Ymr244c-a) with unknown function. We found that the lack of Coa6 causes severe assembly defects of the respiratory supercomplexes. Moreover, we found that the level of monomeric complex IV, but not complex III, is decreased in *coa*6Δ mitochondria, which very likely is the cause of the impaired assembly of supercomplexes. So far Coa6 has not been found as a stoichiometric component of single respiratory complexes or respiratory chain supercomplexes (13, 40, 65, 72). It is therefore more likely that it plays a role as an assembly factor. This is also supported by our observation that the levels of mitochondrial encoded subunits of complex IV are decreased in *coa*6Δ mitochondria, a typical feature observed in mutants with cytochrome *c* oxidase assembly defects (13, 73–75). Thus, we propose Coa6 as a novel assembly factor of the yeast cytochrome *c* oxidase. Coa6 is a homologue of the human open reading frame C1Orf31, a protein of unknown function. Interestingly, a recent bioinformatic study proposed that the human Coa6 homolog C1Orf31 is a putative assembly factor for cytochrome *c* oxidase (76).

Data Availability—All MS data are publicly available via the PRIDE repository (http://www.ebi.ac.uk/pride/) (77, 78), using accession numbers 24150–24184.

Acknowledgments—We thank Drs. Nils Wiedemann, Peter Rehling, and Nikolaus Pfanner for discussion and C. Prinz and B. Schönfisch for expert technical assistance.

* This work was supported by the Deutsche Forschungsgemeinschaft, Excellence Initiative of the German Federal & State Governments (EXC 294 BIOSS; GSC-4 Spemann Graduate School), the international graduate school GRK1478, the Ministerium für Innovation, Wissenschaft und Forschung des Landes Nordrhein-Westfalen, and the Bundesministerium für Bildung und Forschung (Dynamo).

S This article contains supplemental Fig. S1 and Tables S1 to S5.

¶¶ To whom correspondence may be addressed: René Zahedi, Tel.: (49) 231 1392-4143, Fax: (49) 231 1392-4850, E-mail: rene.zahedi@isas.de.

[1] To whom correspondence may be addressed: Chris Meisinger, Tel.: (49) 761 203-5287, Fax: (49) 761 203-5261, E-mail: chris.meisinger@biochemie.uni-freiburg.de.

§ These authors contributed equally to this work.

REFERENCES

1. Reinders, J., Zahedi, R. P., Pfanner, N., Meisinger, C., and Sickmann, A. (2006) Toward the complete yeast mitochondrial proteome: multidimensional separation techniques for mitochondrial proteomics. *J. Proteome Res.* **5,** 1543–1554
2. Meisinger, C., Sickmann, A., and Pfanner, N. (2008) The mitochondrial proteome: from inventory to function. *Cell* **134,** 22–24
3. Pagliarini, D. J., Calvo, S. E., Chang, B., Sheth, S. A., Vafai, S. B., Ong, S. E., Walford, G. A., Sugiana, C., Boneh, A., Chen, W. K., Hill, D. E., Vidal, M., Evans, J. G., Thorburn, D. R., Carr, S. A., and Mootha, V. K. (2008) A mitochondrial protein compendium elucidates complex I disease biology. *Cell* **134,** 112–123
4. Zahedi, R. P., Sickmann, A., Boehm, A. M., Winkler, C., Zufall, N., Schönfisch, B., Guiard, B., Pfanner, N., and Meisinger, C. (2006) Proteomic analysis of the yeast mitochondrial outer membrane reveals accumulation of a subclass of preproteins. *Mol. Biol. Cell* **17,** 1436–1450
5. Schmitt, S., Prokisch, H., Schlunck, T., Camp, D. G., Ahting, U., Waizenegger, T., Scharfe, C., Meitinger, T., Imhof, A., Neupert, W., Oefner, P. J., and Rapaport, D. (2006) Proteome analysis of mitochondrial outer membrane from Neurospora crassa. *Proteomics* **6,** 72–80
6. Duncan, O., Taylor, N. L., Carrie, C., Eubel, H., Kubiszewski-Jakubiak, S., Zhang, B., Narsai, R., Millar, A. H., and Whelan, J. (2011) Multiple lines of evidence localize signaling, morphology, and lipid biosynthesis machinery to the mitochondrial outer membrane of Arabidopsis. *Plant Physiol.* **157,** 1093–1113
7. Riemer, J., Fischer, M., and Herrmann, J. M. (2011) Oxidation-driven protein import into mitochondria: insights and blind spots. *Biochim. Biophys. Acta* **1808,** 981–989
8. Herrmann, J. M., and Riemer, J. (2010) The intermembrane space of mitochondria. *Antioxid. Redox Signal.* **13,** 1341–1358
9. Scorrano, L. (2009) Opening the doors to cytochrome c: changes in mitochondrial shape and apoptosis. *Int. J. Biochem. Cell Biol.* **41,** 1875–1883
10. Martinou, J. C., and Youle, R. J. (2011) Mitochondria in apoptosis: Bcl-2 family members and mitochondrial dynamics. *Dev. Cell* **21,** 92–101
11. Diaz, F., Kotarsky, H., Fellman, V., and Moraes, C. T. (2011) Mitochondrial disorders caused by mutations in respiratory chain assembly factors. *Semin. Fetal Neonatal Med.* **16,** 197–204
12. Smith, P. M., Fox, J. L., and Winge, D. R. (2012) Biogenesis of the cytochrome bc(1) complex and role of assembly factors. *Biochim. Biophys. Acta* **1817,** 276–286
13. Mick, D. U., Fox, T. D., and Rehling, P. (2011) Inventory control: cytochrome c oxidase assembly regulates mitochondrial translation. *Nat. Rev. Mol. Cell Biol.* **12,** 14–20
14. Neupert, W., and Herrmann, J. M. (2007) Translocation of proteins into mitochondria. *Annu. Rev. Biochem.* **76,** 723–749

15. de Marcos-Lousa, C., Sideris, D. P., and Tokatlidis, K. (2006) Translocation of mitochondrial inner-membrane proteins: conformation matters. *Trends Biochem. Sci.* **31,** 259–267
16. Koehler, C. M., and Tienson, H. L. (2009) Redox regulation of protein folding in the mitochondrial intermembrane space. *Biochim. Biophys. Acta* **1793,** 139–145
17. Endo, T., and Yamano, K. (2010) Transport of proteins across or into the mitochondrial outer membrane. *Biochim. Biophys. Acta* **1803,** 706–714
18. Chacinska, A., Koehler, C. M., Milenkovic, D., Lithgow, T., and Pfanner, N. (2009) Importing mitochondrial proteins: machineries and mechanisms. *Cell* **138,** 628–644
19. Schmidt, O., Pfanner, N., and Meisinger, C. (2010) Mitochondrial protein import: from proteomics to functional mechanisms. *Nat. Rev. Mol. Cell Biol.* **11,** 655–667
20. Koppen, M., and Langer, T. (2007) Protein degradation within mitochondria: versatile activities of AAA proteases and other peptidases. *Crit. Rev. Biochem. Mol. Biol.* **42,** 221–242
21. Mossmann, D., Meisinger, C., and Vögtle, F. N. (2011) Processing of mitochondrial presequences. *Biochim. Biophys. Acta* **1819,** 1098–1106
22. Teixeira, P. F., and Glaser, E. (2012) Processing peptidases in mitochondria and chloroplasts. *Biochim. Biophys. Acta* 10.1016/j.bbamcr.2012.03.012
23. Gabriel, K., Milenkovic, D., Chacinska, A., Müller, J., Guiard, B., Pfanner, N., and Meisinger, C. (2007) Novel mitochondrial intermembrane space proteins as substrates of the MIA import pathway. *J. Mol. Biol.* **365,** 612–620
24. Longen, S., Bien, M., Bihlmaier, K., Kloeppel, C., Kauff, F., Hammermeister, M., Westermann, B., Herrmann, J. M., and Riemer, J. (2009) Systematic analysis of the twin cx(9)c protein family. *J. Mol. Biol.* **393,** 356–368
25. Banci, L., Bertini, I., Cefaro, C., Ciofi-Baffoni, S., Gallo, A., Martinelli, M., Sideris, D. P., Katrakili, N., and Tokatlidis, K. (2009) MIA40 is an oxidoreductase that catalyzes oxidative protein folding in mitochondria. *Nat. Struct. Mol. Biol.* **16,** 198–206
26. Mesecke, N., Terziyska, N., Kozany, C., Baumann, F., Neupert, W., Hell, K., and Herrmann, J. M. (2005) A disulfide relay system in the intermembrane space of mitochondria that mediates protein import. *Cell* **121,** 1059–1069
27. Rissler, M., Wiedemann, N., Pfannschmidt, S., Gabriel, K., Guiard, B., Pfanner, N., and Chacinska, A. (2005) The essential mitochondrial protein Erv1 cooperates with Mia40 in biogenesis of intermembrane space proteins. *J. Mol. Biol.* **353,** 485–492
28. Allen, S., Balabanidou, V., Sideris, D. P., Lisowsky, T., and Tokatlidis, K. (2005) Erv1 mediates the Mia40-dependent protein import pathway and provides a functional link to the respiratory chain by shuttling electrons to cytochrome c. *J. Mol. Biol.* **353,** 937–944
29. Roucou, X., Montessuit, S., Antonsson, B., and Martinou, J. C. (2002) Bax oligomerization in mitochondrial membranes requires tBid (caspase-8-cleaved Bid) and a mitochondrial protein. *Biochem. J.* **368,** 915–921
30. Sanjuán Szklarz, L. K., Kozjak-Pavlovic, V., Vögtle, F. N., Chacinska, A., Milenkovic, D., Vogel, S., Dürr, M., Westermann, B., Guiard, B., Martinou, J. C., Borner, C., Pfanner, N., and Meisinger, C. (2007) Preprotein transport machineries of yeast mitochondrial outer membrane are not required for Bax-induced release of intermembrane space proteins. *J. Mol. Biol.* **368,** 44–54
31. Sikorski, R. S., and Hieter, P. (1989) A system of shuttle vectors and yeast host strains designed for efficient manipulation of DNA in Saccharomyces cerevisiae. *Genetics* **122,** 19–27
32. Meisinger, C., Rissler, M., Chacinska, A., Szklarz, L. K., Milenkovic, D., Kozjak, V., Schönfisch, B., Lohaus, C., Meyer, H. E., Yaffe, M. P., Guiard, B., Wiedemann, N., and Pfanner, N. (2004) The mitochondrial morphology protein Mdm10 functions in assembly of the preprotein translocase of the outer membrane. *Dev. Cell* **7,** 61–71
33. Dietmeier, K., Hönlinger, A., Bömer, U., Dekker, P. J., Eckerskorn, C., Lottspeich, F., Kübrich, M., and Pfanner, N. (1997) Tom5 functionally links mitochondrial preprotein receptors to the general import pore. *Nature* **388,** 195–200
34. van Wilpe, S., Ryan, M. T., Hill, K., Maarse, A. C., Meisinger, C., Brix, J., Dekker, P. J., Moczko, M., Wagner, R., Meijer, M., Guiard, B., Hönlinger, A., and Pfanner, N. (1999) Tom22 is a multifunctional organizer of the mitochondrial preprotein translocase. *Nature* **401,** 485–489
35. Chacinska, A., Pfannschmidt, S., Wiedemann, N., Kozjak, V., Sanjuán Szklarz, L. K., Schulze-Specking, A., Truscott, K. N., Guiard, B., Meisinger, C., and Pfanner, N. (2004) Essential role of Mia40 in import and assembly of mitochondrial intermembrane space proteins. *EMBO J.* **23,** 3735–3746
36. Gebert, N., Gebert, M., Oeljeklaus, S., von der Malsburg, K., Stroud, D. A., Kulawiak, B., Wirth, C., Zahedi, R. P., Dolezal, P., Wiese, S., Simon, O., Schulze-Specking, A., Truscott, K. N., Sickmann, A., Rehling, P., Guiard, B., Hunte, C., Warscheid, B., van der Laan, M., Pfanner, N., and Wiedemann N. (2011) Dual function of Sdh3 in the respiratory chain and TIM22 protein translocase of the mitochondrial inner membrane. *Mol. Cell* **44,** 811–818
37. Meisinger, C., Pfanner, N., and Truscott, K. N. (2006) Isolation of yeast mitochondria. *Methods Mol. Biol.* **313,** 33–39
38. Ryan, M. T., Voos, W., and Pfanner, N. (2001) Assaying protein import into mitochondria. *Methods Cell Biol.* **65,** 189–215
39. Schägger, H., and Pfeiffer, K. (2000) Supercomplexes in the respiratory chains of yeast and mammalian mitochondria. *EMBO J.* **19,** 1777–1783
40. Vukotic, M., Oeljeklaus, S., Wiese, S., Vögtle, F. N., Meisinger, C., Meyer, H. E., Zieseniss, A., Katschinski, D. M., Jans, D. C., Jakobs, S., Warscheid, B., Rehling, P., and Deckers, M. (2012) Rcf1 mediates cytochrome oxidase assembly and respirasome formation, revealing heterogeneity of the enzyme complex. *Cell Metab.* **15,** 336–347
41. Olsen, J. V., de Godoy, L. M., Li, G., Macek, B., Mortensen, P., Pesch, R., Makarov, A., Lange, O., Horning, S., and Mann, M. (2005) Parts per million mass accuracy on an Orbitrap mass spectrometer via lock mass injection into a C-trap. *Mol. Cell. Proteomics* **4,** 2010–2021
42. Perkins, D. N., Pappin, D. J., Creasy, D. M., and Cottrell, J. S. (1999) Probability-based protein identification by searching sequence databases using mass spectrometry data. *Electrophoresis* **20,** 3551–3567
43. Eng, J. K., McCormack, A. L., and Yates, J. R. (1996) An approach to correlate tandem mass spectral data of peptides with amino acid sequences in a protein database. *J. Am. Soc. Mass. Spectrom.* **5,** 976–989
44. Geer, L. Y., Markey, S. P., Kowalak, J. A., Wagner, L., Xu, M., Maynard, D. M., Yang, X., Shi, W., and Bryant, S. H. (2004) Open mass spectrometry search algorithm. *J. Proteome Res.* **3,** 958–964
45. Kapp, E. A., Schütz, F., Connolly, L. M., Chakel, J. A., Meza, J. E., Miller, C. A., Fenyo, D., Eng, J. K., Adkins, J. N., Omenn, G. S., and Simpson, R. J. (2005) An evaluation, comparison, and accurate benchmarking of several publicly available MS/MS search algorithms: sensitivity and specificity analysis. *Proteomics* **5,** 3475–3490
46. Vaudel, M., Burkhart, J. M., Sickmann, A., Martens, L., and Zahedi, R. P. (2011) Peptide identification quality control. *Proteomics* **11,** 2105–2114
47. Kessner, D., Chambers, M., Burke, R., Agus, D., and Mallick, P. (2008) ProteoWizard: open source software for rapid proteomics tools development. *Bioinformatics* **24,** 2534–2536
48. Vaudel, M., Barsnes, H., Berven, F. S., Sickmann, A., and Martens, L. (2011) SearchGUI: an open-source graphical user interface for simultaneous OMSSA and X!Tandem searches. *Proteomics* **11,** 996–999
49. Cherry, J. M., Hong, E. L., Amundsen, C., Balakrishnan, R., Binkley, G., Chan, E. T., Christie, K. R., Costanzo, M. C., Dwight, S. S., Engel, S. R., Fisk, D. G., Hirschman, J. E., Hitz, B. C., Karra, K., Krieger, C. J., Miyasato, S. R., Nash, R. S., Park, J., Skrzypek, M. S., Simison, M., Weng, S., and Wong, E. D. (2011) Saccharomyces Genome Database: the genomics resource of budding yeast. *Nucleic Acids Res.* **40,** 700–705
50. Sickmann, A., Reinders, J., Wagner, Y., Joppich, C., Zahedi, R., Meyer, H. E., Schönfisch, B., Perschil, I., Chacinska, A., Guiard, B., Rehling, P., Pfanner, N., and Meisinger, C. (2003) The proteome of Saccharomyces cerevisiae mitochondria. *Proc. Natl. Acad. Sci. U.S.A.* **100,** 13207–13212
51. van der Laan, M., Wiedemann, N., Mick, D. U., Guiard, B., Rehling, P., and Pfanner, N. (2006) A role for Tim21 in membrane-potential-dependent preprotein sorting in mitochondria. *Curr. Biol.* **16,** 2271–2276
52. Yang, M., and Trumpower, B. L. (1994) Deletion of QCR6, the gene encoding subunit six of the mitochondrial cytochrome bc1 complex, blocks maturation of cytochrome c1, and causes temperature-sensitive petite growth in Saccharomyces cerevisiae. *J. Biol. Chem.* **269,** 1270–1275
53. Krause-Buchholz, U., Gey, U., Wünschmann, J., Becker, S., and Rödel, G. (2006) YIL042c and YOR090c encode the kinase and phosphatase of the Saccharomyces cerevisiae pyruvate dehydrogenase complex. *FEBS Lett.* **580,** 2553–2560
54. Stojanovski, D., Bragoszewski, P., and Chacinska, A. (2012) The MIA pathway: a tight bond between protein transport and oxidative folding in mitochondria. *Biochim. Biophys. Acta* **1823,** 1142–1150

55. Milenkovic, D., Ramming, T., Müller, J. M., Wenz, L. S., Gebert, N., Schulze-Specking, A., Rospert, S., and Chacinska, A. (2009) Identification of the signal directing Tim9 and Tim10 into the intermembrane space of mitochondria. *Mol. Biol. Cell* **20,** 2530–2539
56. Kurz, M., Martin, H., Rassow, J., Pfanner, N., and Ryan, M. T. (1999) Biogenesis of Tim proteins of the mitochondrial carrier import pathway: differential targeting mechanisms and crossing over with the main import pathway. *Mol. Biol. Cell* **10,** 2461–2474
57. Stuart, R. A. (2008) Supercomplex organization of the oxidative phosphorylation enzymes in yeast mitochondria. *J. Bioenerg. Biomembr.* **40,** 411–417
58. Acín-Pérez, R., Fernández-Silva, P., Peleato, M. L., Pérez-Martos, A., Enriquez, J. A. (2008) Respiratory active mitochondrial supercomplexes. *Mol. Cell* **32,** 529–539
59. Martin, H., Eckerskorn, C., Gärtner, F., Rassow, J., Lottspeich, F., and Pfanner, N. (1998) The yeast mitochondrial intermembrane space: purification and analysis of two distinct fractions. *Anal. Biochem.* **265,** 123–128
60. Patterson, S. D., Spahr, C. S., Daugas, E., Susin, S. A., Irinopoulou, T., Koehler, C., and Kroemer, G. (2000) Mass spectrometric identification of proteins released from mitochondria undergoing permeability transition. *Cell Death Differ.* **7,** 137–144
61. Jin, C., Barrientos, A., and Tzagoloff, A. (2003) Yeast dihydroxybutanone phosphate synthase, an enzyme of the riboflavin biosynthetic pathway, has a second unrelated function in expression of mitochondrial respiration. *J. Biol. Chem.* **278,** 14698–14703
62. Osman, C., Haag, M., Potting, C., Rodenfels, J., Dip, P. V., Wieland, F. T., Brügger, B., Westermann, B., and Langer, T. (2009) The genetic interactome of prohibitins: coordinated control of cardiolipin and phosphatidylethanolamine by conserved regulators in mitochondria. *J. Cell Biol.* **184,** 583–596
63. Tamura, Y., Endo, T., Iijima, M., and Sesaki, H. (2009) Ups1p and Ups2p antagonistically regulate cardiolipin metabolism in mitochondria. *J. Cell Biol.* **185,** 1029–1045
64. LaMarche, A. E., Abate, M. I., Chan, S. H., and Trumpower, B. L. (1992) Isolation and characterization of COX12, the nuclear gene for a previously unrecognized subunit of Saccharomyces cerevisiae cytochrome c oxidase. *J. Biol. Chem.* **267,** 22473–22480
65. Tsukihara, T., Aoyama, H., Yamashita, E., Tomizaki, T., Yamaguchi, H., Shinzawa-Itoh, K., Nakashima, R., Yaono, R., and Yoshikawa, S. (1996) The whole structure of the 13-subunit oxidized cytochrome c oxidase at 2.8 A. *Science* **272,** 1136–1144
66. Khalimonchuk, O., Rigby, K., Bestwick, M., Pierrel, F., Cobine, P. A., and Winge, D. R. (2008) Pet191 is a cytochrome c oxidase assembly factor in Saccharomyces cerevisiae. *Eukaryot. Cell* **7,** 1427–1431
67. Kumar, A., Agarwal, S., Heyman, J. A., Matson, S., Heidtman, M., Piccirillo, S., Umansky, L., Drawid, A., Jansen, R., Liu, Y., Cheung, K. H., Miller, P., Gerstein, M., Roeder, G. S., and Snyder, M. (2002) Subcellular localization of the yeast proteome. *Genes Dev.* **16,** 707–719
68. Huh, W. K., Falvo, J. V., Gerke, L. C., Carroll, A. S., Howson, R. W., Weissman, J. S., and O'Shea, E. K. (2003) Global analysis of protein localization in budding yeast. *Nature* **425,** 686–691
69. Herrero, E., Ros, J., Bellí, G., and Cabiscol, E. (2008) Redox control and oxidative stress in yeast cells. *Biochim. Biophys. Acta* **1780,** 1217–1235
70. Arevalo-Rodriguez, M., Wu, X., Hanes, S. D., and Heitman, J. (2004) Prolyl isomerases in yeast. *Front. Biosci.* **9,** 2420–2446
71. García-Ramírez, J. J., Santos, M. A., and Revuelta, J. L. (1995) The Saccharomyces cerevisiae RIB4 gene codes for 6,7-dimethyl-8-ribityllumazine synthase involved in riboflavin biosynthesis. Molecular characterization of the gene and purification of the encoded protein. *J. Biol. Chem.* **270,** 23801–23807
72. Strogolova, V., Furness, A., Robb-McGrath, M., Garlich, J., and Stuart, R. A. (2012) Rcf1 and Rcf2, members of the hypoxia-induced gene 1 protein family, are critical components of the mitochondrial cytochrome bc1-cytochrome c oxidase supercomplex. *Mol. Cell. Biol.* **32,** 1363–1373
73. Zambrano, A., Fontanesi, F., Solans, A., de Oliveira, R. L., Fox, T. D., Tzagoloff, A., and Barrientos, A. (2007) Aberrant translation of cytochrome c oxidase subunit 1 mRNA species in the absence of Mss51p in the yeast Saccharomyces cerevisiae. *Mol. Biol. Cell* **18,** 523–535
74. Pierrel, F., Bestwick, M. L., Cobine, P. A., Khalimonchuk, O., Cricco, J. A., and Winge, D. R. (2007) Coa1 links the Mss51 post-translational function to Cox1 cofactor insertion in cytochrome c oxidase assembly. *EMBO J.* **26,** 4335–4346
75. Mick, D. U., Wagner, K., van der Laan, M., Frazier, A. E., Perschil, I., Pawlas, M., Meyer, H. E., Warscheid, B., and Rehling, P. (2007) Shy1 couples Cox1 translational regulation to cytochrome c oxidase assembly. *EMBO J.* **26,** 4347–4358
76. Szklarczyk, R., Wanschers, B. F., Cuypers, T. D., Esseling, J. J., Riemersma, M., van den Brand, M. A., Gloerich, J., Lasonder, E., van den Heuvel, L. P., Nijtmans, L. G., and Huynen, M. A. (2012) Iterative orthology prediction uncovers new mitochondrial proteins and identifies C12orf62 as the human ortholog of COX14, a protein involved in the assembly of cytochrome c oxidase. *Genome Biol.* **13,** 12
77. Vizcaino, J. A., Cote, R., Reisinger, F., Barsnes, H., Foster, J. M., Rameseder, J., Hermjakob, H., and Martens, L. (2010) The Proteomics Identifications Database: 2010 update. *Nucleic Acids Res.* **38,** D736-D742
78. Barsnes, H., Vizcaino, J. A., Eidhammer, I., and Martens, L. (2009) PRIDE Converter: Making proteomics data-sharing easy. *Nat. Biotechnol.* **27,** 598–599